THE JOURNAL OF BIOLOGICAL CHEMISTRY
Vol. 277, No. 16, Issue of April 19, pp. 13563–13568, 2002
Printed in U.S.A.

The Role of the Cross-link His-Tyr in the Functional Properties of the Binuclear Center in Cytochrome *c* Oxidase*

Received for publication, December 20, 2001, and in revised form, January 29, 2002
Published, JBC Papers in Press, February 1, 2002, DOI 10.1074/jbc.M112200200

Eftychia Pinakoulaki‡, Ute Pfitzner§, Bernd Ludwig§, and Constantinos Varotsis‡¶

From the ‡Department of Chemistry, University of Crete, 71409 Heraklion, Crete, Greece and the §Johann Wolfgang Goethe-Universität, Biozentrum N200, Institut für Biochemie, Molekulare Genetik Marie-Curie-Str. 9, D-60439 Frankfurt/M., Germany

Resonance Raman and Fourier transform infrared spectroscopies have been used to study the aa_3-type cytochrome *c* oxidase and the Y280H mutant from *Paracoccus denitrificans*. The stability of the binuclear center in the absence of the Tyr^{280}-His^{276} cross-link is not compromised since heme a_3 retains the same proximal environment, spin, and coordination state as in the wild type enzyme in both the oxidized and reduced states. We observe two C-O modes in the Y280H mutant at 1966 and 1975 cm^{-1}. The 1975 cm^{-1} mode is assigned to a γ-form and represents a structure of the active site in which Cu_B exerts a steric effect on the heme a_3-bound CO. Therefore, the role of the cross-link is to fix Cu_B in a certain configuration and distance from heme a_3, and not to allow histidine ligands to coordinate to Cu_B rather than to heme a_3, rendering the enzyme inactive, as proposed recently (Das, T. K., Pecoraro, C., Tomson, F. L., Gennis, R. B., and Rousseau, D. L. (1998) *Biochemistry* 37, 14471–14476). The results provide solid evidence that in the Y280H mutant the catalytic site retains its active configuration that allows O_2 binding to heme a_3. Oxygenated intermediates are formed by mixing oxygen with the CO-bound mixed-valence wild type and Y280H enzymes with similar Soret maxima at 438 nm.

Cytochrome *c* oxidase (CcO)[1] couples the one-electron oxidation of cytochrome *c* to the four-electron reduction of molecular oxygen and links these electron transfers to proton translocation across the inner mitochondrial membrane, or the bacterial cytoplasmic membrane, respectively (1–6). The enzyme contains four redox-centers; two hemes *a* and three associated copper atoms. Electron injection from cytochrome *c* to the homo-dinuclear copper center, Cu_A, is followed by intramolecular electron transfer, via the low-spin heme *a*, to the binuclear center which contains a high spin heme a_3 and a Cu_B atom. The latter two species serve as the catalytic site where O_2 is reduced to H_2O. The free energy released in the electron-transfer reactions is conserved as an electrochemical proton gradient across the inner mitochondrial membrane and is used ultimately for ATP synthesis.

The crystal structures of mammalian CcO (7–9) and of the soil bacterium *Paracoccus denitrificans* (10, 11) have been determined providing deep insight in the structural properties of the enzyme. The properties of the binuclear center are of particular importance, since the heme a_3/Cu_B center is the site where dioxygen reduction takes place and is the most probable site of the proton-electron coupling (2). One of the unique properties of the binuclear center that were determined by the crystal structure is the covalent link of Tyr^{280} with one of the three histidine ligands of Cu_B, namely His^{276}. (If not stated otherwise, we adopt the residue numbering of *P. denitrificans*.) This specific tyrosine which is located at the end of the proton K-channel is highly conserved among the heme-copper oxidases and since its discovery it has been proposed to posses an important structural as well as functional role. On the basis of the properties of the Y → F mutant of *Rhodobacter sphaeroides*, analyzed by resonance Raman spectroscopy (RR), Rousseau and co-workers (12) proposed that the tyrosine-histidine cross-linking stabilizes the binuclear center. They suggested that in the absence of the His-Tyr cross-link one of the histidines normally bound to Cu_B coordinates to the heme a_3, leaving the binuclear center severely disrupted, and rendering the enzyme inactive. Based on the crystal structure of bovine CcO, Yoshikawa and co-workers (9) proposed a proton transfer mechanism from this tyrosine to ferric peroxide to generate a hydroperoxo adduct, and subsequently the electron transfer from Cu_B^{1+} via the cross-link would cleave the O-O bond of the ferric hydroperoxide. Moreover, other groups have suggested that the tyrosine can serve as a hydrogen atom donor during the cytochrome oxidase/O_2 reaction (3–4, 6, 11, 13). Recently, Babcock and co-workers (14) proposed that Tyr^{280} is the source for both the proton and the electron required in the O-O bond cleavage, and Michel and co-workers (15) proposed that the EPR signal ($g_{iso} \sim 2.0055$) they observed in the cytochrome aa_3/H_2O_2 (*P. denitrificans*) reaction originated from the cross-linked tyrosine.

Structural information of the heme-Cu_B center have been determined from studies of the CO-bound adducts (16–28). In addition to revealing insights concerning the electronic and steric nature of the heme pocket, CO photodissociation studies provided a powerful tool for studying the dynamics and coordination chemistry in the heme-Cu_B pocket after CO photolysis (29–34). RR spectroscopy is a well adapted technique in the study of terminal oxidases, as it enables us to selectively enhance the vibrational modes of the hemes without interference from the protein matrix and thus identify their oxidation, spin, and ligation state by using established marker bands (35–41). Both RR and FTIR spectroscopy have been employed in the study of the carbonmonoxy derivatives of cytochrome aa_3. The vibrational frequencies of the FeCO unit obtained by the two spectroscopic techniques have been identified in different types of heme-copper oxidases, revealing different conformations of

* This work was supported by grants from Alexander von Humboldt-Stiftung (to C. V. and B. L.), Greek Secretariat of Research and Technology 99 (to C. V.), and Deutsche Forschungsgemeinschaft Grant SFB 472 (to B. L.). The costs of publication of this article were defrayed in part by the payment of page charges. This article must therefore be hereby marked "*advertisement*" in accordance with 18 U.S.C. Section 1734 solely to indicate this fact.

¶ To whom correspondence should be addressed. Fax: 30-810393601; E-mail: varotsis@edu.uoc.gr.

[1] The abbreviations used are: CcO, cytochrome *c* oxidase; MV, mixed valence; RR, resonance Raman; FTIR, Fourier transform infrared.

the active site (16–23). The two major conformers found are termed as α- and β-forms and although their functional significance and the origin for the splitting have not been established, it has been demonstrated that in the α-form the frequencies of the ν(Fe-CO) and ν(C-O) deviate from the inverse linear curve that exists between the frequencies of these two modes in histidine-coordinated heme proteins, while in the β-form those frequencies are placed on the curve (17, 22–28). Recently, from the observed pH-dependent conformational changes in the binuclear site it was postulated that the different structures result from a change in the position of the Cu_B atom with respect to the CO due to the presence of one or more ionizable groups (23). Furthermore, it was suggested that the possible candidates are the cross-linked, conserved tyrosine that is adjacent to the oxygen-binding pocket or one of the histidines that coordinate Cu_B.

In an effort to gain additional information on the role of Tyr^{280} in the catalytic function of CcO we have characterized the wild type and histidine mutant (Y280H) of CcO from *P. denitrificans* in the oxidized, reduced, and CO-bound forms by optical absorption, RR, and FTIR spectroscopies. Our studies show that the Cu_B modification by the Y280H mutant results in only slight perturbation of the formyl group of heme a_3. Therefore, the role of the cross-link is not to allow His^{276} (His^{240} in bovine, His^{284} in *Rb. sphaeroides*) to coordinate to Cu_B instead of the heme iron atom, as previously suggested (12), but to hold Cu_B in a certain configuration and distance from heme a_3. Without the cross-linking of Tyr^{280} and His^{276}, the heme pocket retains its active configuration that allows O_2 binding to heme a_3. Upon direct mixing of O_2 to the CO-bound mixed-valence wild-type and Y280H enzymes, oxygenated species with similar Soret maxima at 438 nm are formed, which decay to the resting form of the enzymes.

EXPERIMENTAL PROCEDURES

Wild-type and mutant CcO was purified from *P. denitrificans* according to published procedures (42, 43). The activity of wild-type and mutant CcO has been reported (43). Mammalian CcO was isolated from beef hearts (44). The samples were concentrated to 100–150 μM in 50 mM Hepes, pH 7.4, containing 0.1% dodecyl β-D-maltoside and stored in liquid nitrogen until use. The fully reduced CO derivative was prepared by flushing CO gas anaerobically to dithionite-reduced enzyme. The mixed-valence CO-bound enzyme was prepared by exposing an anaerobic solution of the resting enzyme to CO for 10 h. RR spectra were obtained from 30 to 40 μM samples in an anaerobic cylindrical quartz spinning cell. The RR spectra were acquired by using a SPEX 1877 triplemate with an EG&G (model 1530-CUV-1024S) CCD detector. A Coherent Innova K-90 Krypton ion laser was used to provide the excitation wavelength of 413.1 nm. A Coherent 590 dye laser connected with a Coherent Innova 200 argon laser was used to provide the excitation wavelength of 431 nm. The power incident on the CcO sample was typically 4–6 mW. FTIR spectra were obtained from 200 to 300 μM samples with a Bruker Equinox 55 FTIR spectrometer equipped with liquid nitrogen-cooled MCT detector. The samples were loaded anaerobically into a cell with CaF_2 windows and a 0.025-mm spacer. The spectra were obtained as difference, using the buffer as background, and each spectrum is the average of 1000 scans. The spectral resolution used for the FTIR measurements was 2 cm^{-1} for the wild-type CO spectrum and 4 cm^{-1} for the Y280H mutant, respectively. Optical absorbance spectra were recorded before and after FTIR and Raman measurements to assess sample stability with a PerkinElmer Life Science Lamda 20 UV-visible spectrometer.

RESULTS AND DISCUSSION

The optical absorption spectra of resting (as isolated) and fully reduced aa_3 from *P. denitrificans* display maxima at 423 and 598 nm in resting form (Fig. 1*A*, *trace a*), and at 444 and 605 nm in the reduced form (Fig. 1*A*, *trace b*). The difference CO-bound-reduced spectrum displays a positive band at 430 nm and a shoulder at 416 nm with a trough at 449 nm (Fig. 1*A*, *trace c*). The optical spectrum of the resting Y280H mutant

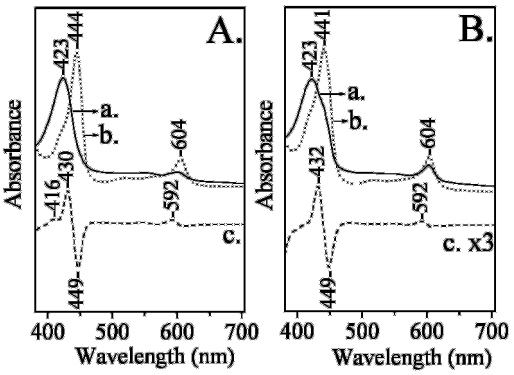

FIG. 1. **Optical absorption spectra of the wild-type cytochrome aa_3 from *P. denitrificans* (*panel A*) and the Y280H mutant (*panel B*) in the "as isolated" (*trace a*, *solid line*) and the dithionite reduced (*trace b*, *dot line*) forms.** In both panels the difference spectrum (*trace c*, *dashed line*) of the reduced CO-bound form minus the reduced indicates the binding of CO to heme a_3. The concentration of the enzyme was 10 μM and the path-length of the cell was 0.5 cm.

shown in Fig. 1*B* (*trace a*) shows in addition to the 423-nm band a shoulder at 441 nm in the Soret region and an increased absorption of the 604-nm band. This indicates that a sizeable percentage of heme *a* (~30%) is reduced in the mutant. Addition of dithionite to Y280H (Fig. 1*B*, *trace b*) shifts the maxima at 441 and 604 nm, consistent with the maxima of the fully reduced wild-type enzyme. The difference spectrum of the reduced CO-bound minus reduced form is characteristic of CO binding to heme a_3, as denoted by the peaks at 432 and 592 nm (Fig. 1*B*, *trace c*).

The high frequency region of the RR spectrum of the resting and reduced wild-type, which are shown in Fig. 2*A* (*traces a* and *b*), are in agreement with those previously reported for heme-copper oxidases (35–37, 39, 40). In the spectrum of the resting enzyme, the oxidation state marker υ_4 is at 1371, establishing that both hemes are in the ferric (Fe^{3+}) state. The modes at 1477 and 1498 cm^{-1} originating from ν_3 of high-spin heme a_3 and low spin heme *a*, respectively, indicate that both hemes are six-coordinate. This is also consistent with structural data which indicate that in this form of the enzyme heme *a* is coordinated by two histidine ligands and that there is a bridging ligand between heme a_3 and Cu_B (10, 11). The core expansion region shows two vibrations at 1572 cm^{-1} (high-spin heme a_3^{3+}) and 1584 cm^{-1} (low-spin heme a^{3+}). The 1612 and 1635 cm^{-1} modes arise from ν_{10} of heme a_3^{3+} and heme a^{3+}, respectively. The 1646 and 1671 cm^{-1} modes have been assigned as the C=O stretching vibrations of the formyl groups (−CHO) of heme a^{3+} and heme a_3^{3+}, respectively (39, 40). The spectrum from the fully reduced enzyme (Fig. 1*A*, *trace b*) has the oxidation state marker, ν_4, at 1359 cm^{-1} indicating that both hemes are in the ferrous state. The modes at 1464 and 1490 cm^{-1} originate from the ferrous, five-coordinate high spin heme a_3^{2+} and the ferrous six-coordinate low-spin heme *a*, respectively. The mode at 1519 originates from ν_{19} of heme a^{2+}. The modes at 1569 and 1584 cm^{-1} originate from ν_2 of heme a_3^{2+} and heme *a*, respectively. The 1612 and 1662 have been assigned as the C=O stretching vibrations of the formyl group (−CHO) of heme a^{2+} and heme a_3^{2+}, respectively (35, 40). The 1623 cm^{-1} mode arises from the C=C stretching vibration of heme a^{2+} and heme a_3^{2+}. The spectral perturbations caused by the Y280H mutation are very limited except for the decrease in intensities of the heme a^{3+} modes and the concomitant appearance of modes originating from a fraction of heme a^{2+} (Fig. 2*B*, *trace a*). The reduction of heme *a* is apparent from the increase in intensities of ν_4 at 1356, ν_{11} at 1519, ν_2 at 1584, ν_{10} at 1612 cm^{-1}, as well the decrease in intensity of the formyl stretching

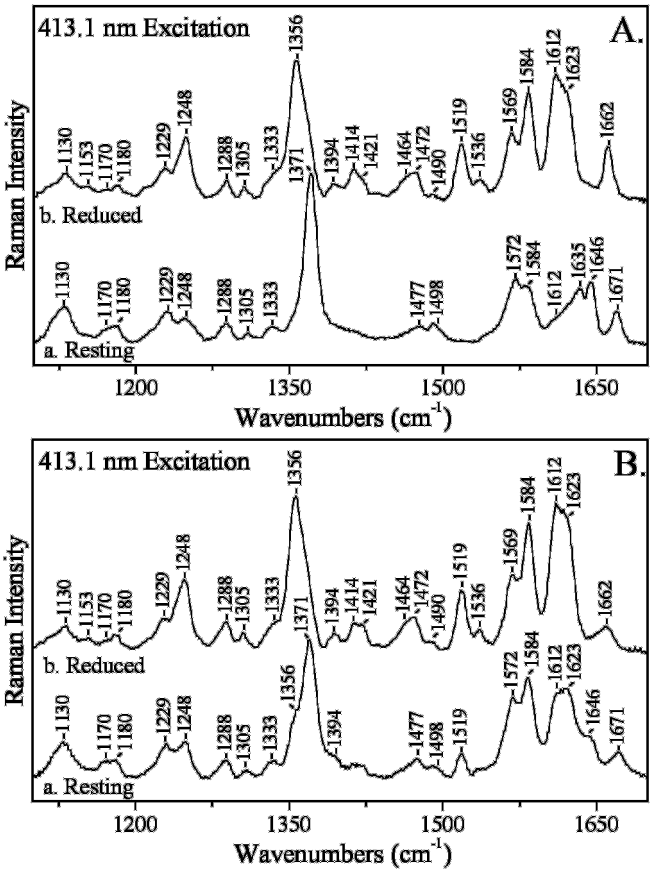

FIG. 2. **High frequency resonance Raman spectra of the wild-type cytochrome aa_3 from *P. denitrificans* (*panel A*) and the Y280H mutant (*panel B*) in the resting (*trace a*) and the dithionite reduced (*trace b*) forms.** The excitation laser wavelength was 413.1 nm. The accumulation time was 15 min for each spectrum.

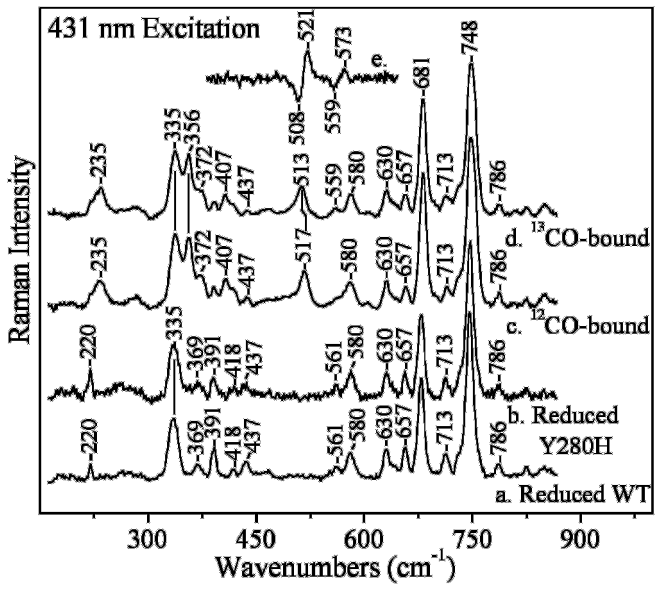

FIG. 3. **Resonance Raman spectra of the reduced wild-type cytochrome aa_3 from *P. denitrificans* (*trace a*) and the Y280H mutant (*trace b*) in the low frequency region.** The reduced wild-type complex with ^{12}CO and ^{13}CO are shown in *traces c* and *d*, respectively. The difference spectrum ^{12}CO-^{13}CO is shown in *trace e*. The excitation laser wavelength was 431 nm. The accumulation time was 20 min for each spectrum.

vibration at 1646 cm^{-1}. All the modes associated with the high spin heme a_3^{3+} are very similar to those of the wild-type enzyme. The only exception is the reduced intensity of the formyl stretching vibration at 1671 cm^{-1}. The RR spectrum of the fully reduced Y280H enzyme (Fig. 2*B*, *trace b*) is very similar to that of the fully reduced wild-type, with the exception of the formyl vibration at 1662 cm^{-1} which is weaker in the mutant.

No unusual stereochemical influences on heme a_3 are apparent in the Y280H mutant that would modify the heme a_3 ligand-binding site. In addition, no evidence for any histidine coordination from Cu_B to heme a_3 is apparent. Thus, our data do not support the conclusions of Das *et al*. (12) that, without the cross-linking of Tyr^{288} and His^{284} (*R. sphaeroides* residue numbering), the heme pocket becomes severely disrupted and one of the histidines bound to Cu_B coordinates to heme a_3, lowering its redox potential.

Fig. 3 shows the low-frequency RR spectra of the fully reduced wild-type and Y280H mutant, and that of the wild-type CO-bound form. The RR spectrum of the fully reduced enzyme (*trace a*) is characterized by the Fe-His stretching mode at 220 cm^{-1} and porphyrin modes of both hemes *a* and a_3. Very similar spectra were obtained for the Y280H mutant as shown in *trace b*. The Fe-His stretching mode is 6 cm^{-1} higher in *P. denitrificans* than it is in CcO (36). The binding of CO to heme a_3^{2+} is accompanied by the disappearance of the Fe-His stretching vibration at 220 cm^{-1} and of the porphyrin mode at 369 cm^{-1} (*trace c*). In the 400–600 cm^{-1} region of the RR spectrum of the CO complex, one frequency for ν(Fe-CO) is detected at 517 cm^{-1}. Assignment of this frequency is confirmed by isotope (^{13}CO) replacement experiment (*trace d*), where the corresponding line appears at 513 cm^{-1}, close to the value expected for a two-harmonic oscillator between iron and CO. The difference spectrum (*trace e*) confirms the above assignment. In the ^{13}CO-bound adduct we also detect a line at 559 cm^{-1}. Although the presence of a porphyrin mode at ~580 cm^{-1} partially obscures band assignment with ^{12}CO in this region, the difference spectrum shows that the 559 cm^{-1} band shifts to 573 cm^{-1} when the experiment is repeated with ^{12}CO. We assign the 573 cm^{-1} mode to the Fe-C-O bending mode δ(Fe-C-O). The frequencies of the 517 and 573 cm^{-1} modes are similar to those that have been reported for the aa_3-type oxidases from beef heart (16), *R. sphaeroides* (17), and aa_3-*600* from *Bacillus subtilis* (21).

The increased frequency of the Fe-His mode we observe in the aa_3 from *P. denitrificans* can be attributed to the strength of the H-bond of the proximal His^{411} ligand to Gly^{387} (41). From the model compound work, the complex with a weaker (or absent) hydrogen bond to the proximal His is expected to have the weaker Fe-His bond and the lower frequency vibration (36). The observation of the Fe-His at 220 cm^{-1} in conjunction with the high frequency data further supports our conclusion that heme a_3^{2+} in the Y280H mutant is five-coordinated, high-spin, and the proximal environment of heme a_3^{2+} in the mutant behaves in a manner analogous to the wild type. Since The Fe-His^{411} forms the only covalent linkage between the five-coordinate heme a_3 and the protein, protein structural changes should be manifested through this bond. From the absence of such changes in the proximal environment of heme a_3^{2+}, any protein structural change due to the mutation is not widespread but is more localized in the Cu_B environment.

Structural information such as the geometry of the bound CO to the heme and its interactions with Cu_B has been determined from the vibrational modes involving the CO. Although the ν(Fe-CO) and δ(Fe-C-O) we have observed is similar to other aa_3-type oxidases, the $I_\delta/I_\nu \sim 0.25$ we observe is low compared with those of CcO and *R. sphaeroides* aa_3-type oxidase ($I_\delta/I_\nu = 0.43$) and significantly higher than that of cytochrome bo_3 (20) ($I_\delta/I_\nu = 0.1$). It has been argued that a high I_δ/I_ν is an indication of a strong interaction between the CO

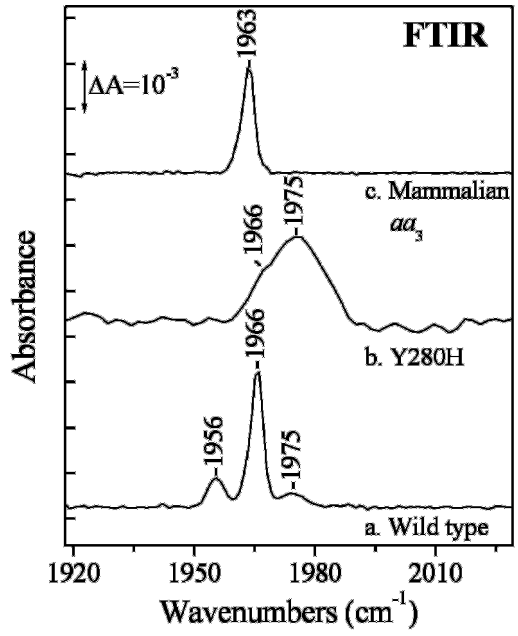

FIG. 4. **FTIR spectra of the fully reduced CO derivative of wild type cytochrome aa_3 from *P. denitrificans* (*trace a*) and of the Y280H mutant (*trace b*).** For comparison the spectrum of the CO derivative of mammalian aa_3 is depicted in *trace c*.

and Cu_B. Consequently, our data suggest that the Fe . . . Cu_B distance is longer in our case. However, despite the increased Fe-Cu_B distance we have not been able to detect a low-energy Fe-C bond (~490 cm^{-1}) corresponding to the high energy C-O bond (~1950 cm^{-1}) of the β-conformer. Recently, it was postulated that the two distinctly different Fe-CO modes observed in the RR of the *Rb. sphaeroides* spectra result from a change in the position of Cu_B with respect to the CO due to the presence of one or more ionizable groups in the vicinity of the binuclear center (23). Additional experiments are in progress in our laboratory to address this possibility in the aa_3 oxidase from *P. denitrificans*.

Fig. 4 shows the FTIR spectra of the CO-bound wild-type and Y280H mutant of aa_3 from *P. denitrificans* at room temperature. For comparison, the fully reduced aa_3-CO complex of the mammalian enzyme is included (*trace c*). *Trace a*, shows that the C-O stretching modes from the *P. denitrificans* aa_3 enzyme split into three components just as was found in the low-temperature experiments (27). The major component is centered at 1966 cm^{-1} (α-form) and two minors are located at 1956 cm^{-1} (β-form) and 1975 cm^{-1}. The frequency of the major CO stretching mode at 1966 cm^{-1}, which we detect in *P. denitrificans* is 3 cm^{-1} higher than the corresponding frequency of the CO-bound heme a_3 of CcO (*trace c*). *Trace b* shows that the Y280H mutant has two conformers that have ν(CO) at 1966 and 1975 cm^{-1}. Similar results have been obtained in the low-temperature experiments.[2]

The structural basis for the splitting of the enzyme into the α- and β-forms has not been determined and no information regarding the origin of the 1975 cm^{-1} has been reported. The FWHM is ~5 cm^{-1} in the C-O modes of the major conformer in both the mammalian and *P. denitrificans* enzymes indicating the absence of a wide distribution of allowed CO conformations. Thus, these data confirm the similarity in the properties of the active sites in these two terminal oxidases. The presence of the 1956 and 1975 cm^{-1} modes in the *P. denitrificans* do indicate, however, that the binuclear site of the bacterial enzyme, while similar, is not identical to its mammalian counterpart. Conversion between the α- and β-forms is pH-dependent and has been attributed to changes in the iron-copper distance (23). It has also been demonstrated from the low-temperature FTIR data that the amplitudes of the bands attributed to the α- and β-forms are temperature and pH-dependent (27). Thus the α-form represents a constricted pocket that will not allow CO to coordinate to heme iron without strong distal polar interactions between the CO and the copper atom, while in the β-form the Cu_B atom is moved away from the bound CO. Based on the above interpretation regarding the origin of the α- and β-forms we assign the 1975 cm^{-1} mode to the γ-conformation in which Cu_B is moved closer to the CO-bound heme a_3, thereby the Fe-C-O moiety is further distorted from its preferred symmetry in the α-form. Unlike the wild-type enzyme which has a prominent α-form, the mutant enzyme exhibits the 1975 cm^{-1} (γ-form)/1966 cm^{-1}(α-form) in a 1.8 ratio indicating that the γ-confomer is the major confomer in the mutant. Consequently, in the absence of the cross-link Tyr-His, the Cu_B atom has moved further closer to the CO-bound heme a_3. This is further supported by the absence of the β-form (1956 cm^{-1}) in the mutant enzyme in which the CO is bound without anomalous polar or steric interactions. Both C-O stretches for the Y280H mutant are broad indicating a wide distribution of allowed CO conformations. In the absence of Tyr^{280}, the heme a_3-Cu_B distance has changed and Cu_B is not fixed in a certain position resulting in different Cu_B conformations. The different conformations of Cu_B in the mutant reflect significant differences in the heme environment, thereby alter the properties of the CO modes observed in the FTIR spectra. In the CO derivatives, the different conformations of Cu_B could easily cause the change in the C-O frequency and bandwidth since it is well established that ligand frequencies and bandwidths in heme proteins are modulated by the properties of the distal environment.

It has been established by Rousseau *et al*. (12, 16–18, 20) that the ν(Fe-CO) and ν(CO) frequencies of heme proteins and the correlation between them reflect: (*a*) the identity and properties of the proximal ligand because the bound CO competes with the proximal ligand for the same iron d_z^2 orbital, and (*b*) indicate the polarity of the distal heme pocket. A highly polar environment favors π-back donation, resulting in an increased ν(Fe-CO) and reduced ν(C-O) due to the increased density in the CO antibonding orbitals. Additional information concerning the properties of the proximal environment in heme-copper oxidases and how it influences the ligand properties on the distal site has been deduced from the unique inverse linear correlation that exists between the frequencies of Fe-His and the Fe-CO stretching modes. Recently, we have shown that in heme-Cu_B oxidases the strength of the proximal histidine H-bonding interaction affects the strength of both the Fe-C and C-O bonds which are further influenced by the Cu_B distal environment (21). We consider both proximal and distal effects on the origin of the ν(Fe-CO) and ν(CO) frequencies we have observed.

The ~4 cm^{-1} downshift in the ν(Fe-CO) of *P. denitrificans*, when compared with that found in CcO, is brought about by a stronger hydrogen bonding interaction of the proximal histidine, and by distal effects on the heme a_3-bound CO exerted by Cu_B. This argument is supported by the observed high frequency of the Fe-His stretching mode at 220 cm^{-1}, as compared with aa_3- and bo_3-type oxidases. A similar conclusion concerning the effect of the proximal ligand to the properties of the distal CO was reached recently by Wang and co-workers (45) for prostaglandin H synthase. On the other hand, Das *et al*. (23) has argued recently that the pH dependence of the Fe-C-O modes they observed in *Rb. sphaeroides* cannot be attributed to

[2] P. Hellwig, submitted for publication.

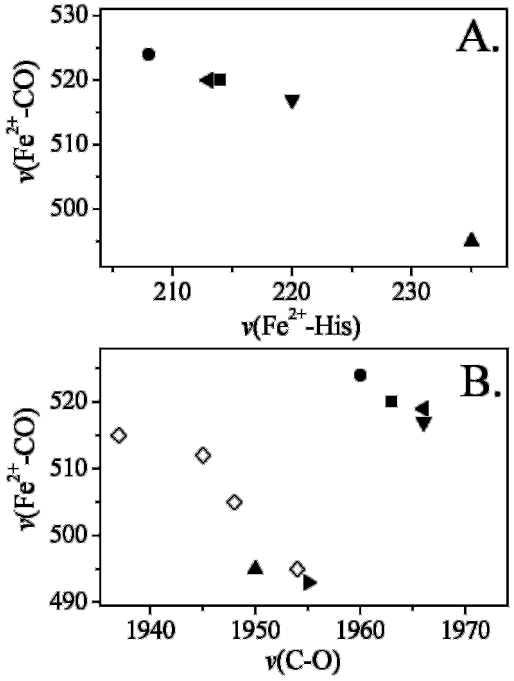

FIG. 5. ***Panel A*, correlation between frequencies of the Fe-His *versus* C-O stretching modes.** *Filled circle*, cytochrome bo_3 from *E. coli*; *filled left pointed arrow*, the α-form of cytochrome aa_3 from *R. sphaeroides*; *filled square*, mammalian cytochrome *c* oxidase and cytochrome aa_3 from *B. subtilis*; *filled downward pointed arrow*, cytochrome aa_3 from *P. denitrificans*; *filled upward pointed arrow*, cytochrome cbb_3 from *R. capsulatus*. *Panel B*, correlation between frequencies of the Fe-CO *versus* C-O stretching modes. Same as in *panel A*, and *filled right pointed arrow*, the β-form of cytochrome aa_3 from *R. sphaeroides*; *open diamond*, myoglobins and hemoglobins.

proximal effects due to the absence of any significant pH-dependent change of the proximal Fe-His stretching frequency. The proximal protein pocket in heme a_3 appears to be hydrophobic and inaccessible to solvent as indicated by Raman studies in D_2O (41). Consequently, the invariance of the frequency of the Fe-His does not necessarily rule out a hydrogen bond interaction to the proximal histidine of heme a_3^{3+}. This is further supported from the crystal structure of the *P. denitrificans* enzyme where it is shown that the proximal His to heme a_3 is indeed hydrogen-bonded to Gly^{387}. The frequencies of the Fe-His and Fe-CO of the enzyme place it on the correlation curve shown in Fig. 5*A*, and posit that it has the same structure as that of the major α-form of the mammalian and *Rb. sphaeroides* enzymes. In the absence of a proximal effect as indicated by the strength of the Fe^{2+}-His located at 220 cm^{-1} in the mutant, the anomalously high C-O stretching mode we observed in the CO-bound Y280H mutant is attributed solely to distal effects. Proximal effects should not be taken under consideration since the Fe-His stretching frequency remains unaffected by the mutation, evidence that a global conformational change is unlikely to have taken place.

The properties of the heme a_3-Cu_B binuclear center have been determined from the correlation of ν(Fe-CO) and ν(C-O) frequencies. The major component (α-form) of the wild-type aa_3, shown in Fig. 5*B*, deviates from the inverse linear correlation curve that exists between the frequencies of ν(Fe-CO) and ν(C-O) between histidine coordinates proteins but fits to the curve of the rest of the terminal oxidases. Although we were unable to detect the ν(Fe-CO) in the β-form, the frequency of the ν(C-O) in the β-form is identical to that reported for the β-form of aa_3 from *Rb. sphaeroides* suggesting that in *P. denitrificans* the frequencies of the β-form are placed on the curve of the histidine-coordinated proteins in which CO can bind to the iron without anomalous polar and steric interactions.

The overall similarity between the frequencies and relative enhancements for the vibrational resonances of oxidized heme a_3 in the wild-type and Y280H mutant indicates that the protein milieu surrounding the heme a_3 is the same in these two forms. A comparison of the high-frequency resonance Raman spectra of the mutant enzyme with that of the wild type, upon reduction, shows no significant differences. However, a conformational change is likely to occur in the binuclear center as indicated by the differences in the intensity and bandwidth of the formyl line of a_3 in both oxidation states of the heme a_3 in the Y280H mutant compared with the wild-type enzyme. This, nevertheless, cannot be attributed to a different oxidation, spin, or ligation change since we have established that no such changes occur as a result of the mutation. Therefore, other possibilities should be considered.

In the absence of a conformational change in heme a_3 the only possibility to account for the reduced intensity of the heme a_3 formyl group is the histidine ligands coordinated to Cu_B. His^{276} is the histidine that forms the cross-link with Tyr^{280} in the wild-type and is not close to the formyl group, thus it is unlikely that it can interact with the formyl group. His^{325} and His^{326} are on the same helix and are close to the formyl group. The closest residue to the formyl oxygen atom of heme a_3 is His^{325} (His^{290} in bovine). It is noteworthy that the absence of Tyr^{280} in the heme pocket results in the loss of the hydrogen-bonding interaction between the hydroxy group on the farnesyl chain of heme a_3 and the hydroxy group on the tyrosine. If the observed changes were due to a change in the hydrogen bonding state of the formyl group then, a frequency shift would have been expected (46). We postulate that changes in the Fe-Cu_B distance could modulate the position of His^{325} with respect to the formyl group. Since no frequency shift is observed, we postulate that the intensity difference is due to a change in the geometry of the formyl group that does not allow the electronic coupling between the formyl group and the porphyrin core to be as effective as in heme a_3 of the wild type enzyme. The complete absence of the C=O stretching vibration of the formyl group (−CHO), reported in the reduced form of the Y280F mutant from *Rb. sphaeroides*, was attributed to an altered heme a_3 conformation. The question arising is whether the change in the orientation of the formyl, which is more evident in the Y280F mutant from *Rb. sphaeroides* than the Y280H aa_3 from *P. denitrificans*, could have an effect in the catalytic function of the enzyme. Recently, Das *et al*. (46) reported a redox-link deprotonation event at the binuclear site of the quinol oxidase from *Acidianus ambivalens*, in which the changes in heme a_3 formyl C-O stretching mode upon heme reduction were attributed to a change in H-bonding to the formyl group. As a possible candidate for the pH-dependent changes they observed suggested His^{290} (bovine sequence numbering) and discussed the implications for proton translocation. However, since this is a single observation and no similar observation has been made for any other aa_3 CcO we cannot consider that the small conformational change we detect in the formyl group of heme a_3 in the Y280H mutant will influence the functional properties of the binuclear center.

Oxygenated intermediate(s) that occur after the decay of the oxyintermediate (I_m) in the MV/O_2 reaction may be generated by direct mixing of oxygen with the CO-bound MV oxidase. These species have been observed by others to have relatively long lifetimes, and thus, they can be studied in a conventional absorption spectrometer. The Soret region optical absorption spectra of oxygenated species formed this way are shown in Fig. 6. The difference spectrum (MV-CO minus oxidized) of the

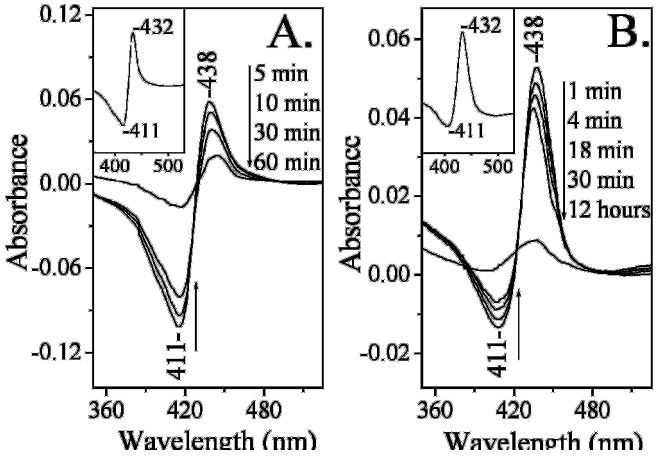

FIG. 6. **Optical absorption difference spectra showing reaction products minus the resting form of wild-type (*panel A*) and Y280H (*panel B*) enzymes at the indicated times.** The reaction was initiated by mixing O_2 with CO-MV-wild-type and -Y280H enzymes. The *insets* show the CO-MV-wild-type and -Y280 enzymes minus their resting forms. The concentration of the enzymes was 10 μM, and the path-length of the cell was 0.5 cm.

wild-type enzyme (*panel A*, *inset*), with maxima and minima at 432 and 411 nm, agrees with that of the CO-bound MV Y280H enzyme (*panel B*, *inset*). In both the wild-type and Y280H MV enzymes, mixing with O_2 shifts the Soret maximum to 438 nm (1–18 min). This indicates that in both the wild-type and mutant enzymes O_2 spontaneously replaces CO. The progression of changes in the Soret indicates that the decay of the oxygenated 438-nm species to the pulsed and subsequently to the resting form occurs on a time scale of tens of seconds. These results suggest that Tyr^{280} is not involved in the formation and decay of the 438-nm species because similar observations were obtained in the wild-type and mutant enzymes. Similar observations in the decay of II_m to the resting form have been reported in the bovine MV CcO/O_2 reaction by Rousseau and co-workers (47). It was also demonstrated by the same authors that intermediates formed by mixing O_2 with CO-bound MV CcO and allowing O_2 to spontaneously replace CO are the same as those of II_m formed in the flow-flash-probe experiments (47).

The data reported here have shown that the cross-link His-Tyr generates a unique environment around Cu_B and holds it in a certain distance and position from heme a_3. In the absence of the cross-linking, Cu_B moves further toward the heme a_3 in the CO bound form of the enzyme, affecting the properties of the bound ligands to heme a_3. Thus, in the Y280H mutant, heme a_3 retains its proximal His ligand and can be oxidized by oxygen. The oxidation of heme a_3 in the Y280H mutant and in the wild-type proceeds through oxygenated species with Soret maxima at 438 nm. The nature of the bound oxygen intermediates following the oxy species remains to be determined. The characterization of the functional/structural implications to the heme a_3-Cu_B center by the Y280H mutation reported here, and the determination of the initial electron transfer steps in the Y280H/O_2 reaction will lead to a better understanding of the oxidative phase of cytochrome *c* oxidase. These experiments are in progress in our laboratory.

Acknowledgment—We thank Werner Müller for excellent technical assistance.

REFERENCES

1. Wikström, M. (1989) *Nature* **338,** 776–778
2. Babcock, G. T., and Wikström, M. (1992) *Nature* **356,** 301–309
3. Michel, H. (1998) *Proc. Natl. Acad. Sci. U. S. A.* **95,** 12819–12824
4. Michel, H. (1998) *Biochemistry* **38,** 15129–15140
5. Ferguson-Miller, S., and Babcock, G. T. (1996) *Chem. Rev.* **96,** 2889–2907
6. Gennis, R. B. (1998) *Biochim. Biophys. Acta* **1365,** 241–248
7. Tsukihara, T., Aoyama, H., Yamashita, E., Tomizaki, T., Yamaguchi, H., Shinzawa-Itoh, K., Nakashima, R., Yaono, R., and Yoshikawa, S. (1995) *Science* **269,** 1069–1074
8. Tsukihara, T., Aoyama, H., Yamashita, E., Tomizaki, T., Yamaguchi, H., Shinzawa-Itoh, K., Nakashima, R., Yaono, R., and Yoshikawa, S. (1996) *Science* **272,** 1136–1144
9. Yoshikawa, S., Shinzawa-Itoh, K., Nakashima, R., Yaono, R., Yamashita, E., Inoue, N., Yao, M., Fei, M. J., Libeu, C. P., Mizushima, T., Yamaguchi, H., Tomizaki, T., and Tsukihara, T. (1998) *Science* **280,** 1723–1729
10. Iwata, S., Ostermeier, C., Ludwig, B., and Michel, H. (1995) *Nature* **376,** 660–669
11. Ostermeier, C., Harrenga, A., Ermler, U., and Michel, H. (1997) *Proc. Natl. Acad. Sci. U. S. A.* **94,** 10547–10553
12. Das, T. K., Pecoraro, C., Tomson, F. L., Gennis, R. B., and Rousseau, D. L. (1998) *Biochemistry* **37,** 14471–14476
13. Proshlyakov, D. A., Pressler, M. A., and Babcock G. T. (1998) *Proc. Natl. Acad. Sci. U. S. A.* **95,** 8020–8025
14. Proshlyakov, D. A., Pressler, M. A., DeMaso, C., Leykam, J. F., DeWitt, D. L., and Babcock, G. T. (2000) *Science* **290,** 1588–1591
15. MacMillan, F., Kannt, A., Behr, J., Prisner, T., and Michel, H. (1999) *Biochemistry* **38,** 9179–91884
16. Argade, P. V., Ching, Y. C., and Rousseau, D. (1984) *Science* **225,** 329–331
17. Wang, J., Takahashi, S., Hosler, P. H., Mitchell, D. M., Ferguson-Miller, S., Gennis, R. B., and Rousseau, D. L. (1995) *Biochemistry* **34,** 9819–9825
18. Wang, J., Gray, K. A., Daldal, F., and Rousseau, D. L. (1995) *J. Am. Chem. Soc.* **117,** 9363–9364
19. Wang, J., Takahashi, S., and Rousseau, D. L. (1995) *Proc. Natl. Acad. Sci. U. S. A.* **92,** 9402–9406
20. Wang, J., Ching, Y-C., Takahashi, S., Rousseau, D. L., Hill, J. J. Rumbley, J., and Gennis, R. B. (1993) *J. Am. Chem. Soc.* **115,** 3390–3391
21. Varotsis, C., and Vamvouka, M. (1998) *J. Phys. Chem. B* **102,** 7670–7673
22. Hosler, P. H., Kim, Y., Shapleigh, J. P., Gennis, R. B., Alben, J. O., Ferguson-Miller, S., and Babcock, G. T. (1994) *J. Am. Chem. Soc.* **116,** 5515–5516
23. Das, T. K., Tomson, F. K., Gennis, R. B., Gordon, M., and Rousseau, D. L. (2001) *Biophys. J.* **80,** 2039–2045
24. Park, S., Pan, L-P., Chan, S. I., and Alben, J. (1996) *Biophys. J.* **71,** 1036–1047
25. Iwase, T., Varotsis, C., Shinzawa-Itoh, K., Yoshikawa, S., and Kitawaga, T. (1999) *J. Am. Chem. Soc.* **121,** 1415–1416
26. Mitchell, D. M., Shapleigh, J. P., Archer, A. M., Alben, J. O., and Gennis, R. B. (1996) *Biochemistry* **35,** 9446–9450
27. Rost, B., Behr, J., Hellwig, P., Richter, O.-M. H., Ludwig, B., Michel, H., and Mäntele, W. (1998) *Biochemistry* **38,** 7565–7571
28. Puustinen, A., Bailey, J. A., Dyer, R. B., Mecklenberg, S. L, Wikström, M., and Woodruff, W. H. (2000) *Biochemistry* **39,** 13195–13200
29. Dyer, R. B., Einarsdóttir, O., Killough, P. M., Lopez-Garriga, J. J., and Woodruff, W. H (1989) *J. Am. Chem. Soc.* **111,** 7657–7659
30. Woodruff, W. H. (1993) *J. Bioenerg. Biomembr.* **25,** 177–188
31. Dyer, R. B., Peterson, K. A., Stoutland, P. O., and Woodruff, W. H. (1994) *Biochemistry* **33,** 500–507
32. Lemon, D. D., Calhoun, M. W., Gennis, R. B., and Woodruff, W. W. (1993) *Biochemistry* **32,** 11953–11956
33. Varotsis, C., Kreszowski, D. H., and Babcock, G. T. (1996) *Biospectroscopy* **2,** 331–338
34. Schelvis, H., Varotsis, C., Deinum, G., Ferguson-Miller S., and Babcock, G. T. (1997) *J. Am. Chem. Soc* **119,** 8409–8416
35. Babcock, G. T. (1988) in *Biological Applications of Raman Spectroscopy* (Spiro, T. G., eds) Vol. 3, pp. 293–346, Wiley, New York
36. Kitagawa, T. (1988) in *Biological Applications of Raman Spectroscopy* (Spiro, T. G., ed) Vol. 3, pp. 97, Wiley, New York
37. Ching, Y-C., Argade, P. V., and Rousseau, D. L. (1985) *Biochemistry* **24,** 4938–4946
38. Varotsis, C., Babcock, G. T., Garcia-Horsmann, A., and Gennis, R. B. (1995) *J. Phys. Chem.* **99,** 16817–16820
39. Vamvouka, M., Müller, W., Ludwig, B., and Varotsis, C. (1999) *J. Phys. Chem.* **103,** 3030–3034
40. Heibel, G. E., Hildebrand, P., Ludwig, B., Steinrücke, P. Soulimane, T., and Buse, G. (1993) *Biochemistry* **32,** 10866–10877
41. Lauraeus, M., Wikström, M., Varotsis, C., Tecklenburg, M. J., and Babcock, G. T. (1992) *Biochemistry* **31,** 10054–10060
42. Hendler, R. W., Pardhasaradhi, K., Reynafarje, B., and Ludwig, B. (1991) *Biophys. J.* **60,** 415–423
43. Pfitzner, U., Odenwald, A., Ostermann, T., Weingard, L., Ludwig, B., and Richter, O.-M. H. (1998) *J. Bioenerg. Biomembr.* **30,** 89–97
44. Varotsis, C., and Babcock, G. T. (1990) *Biochemistry* **29,** 7357–7362
45. Lou, B-S., Snyder, J. K., Marshall, P., Wang, J-S., Wu, G., Kulmacz, R., Tsai, A-L., and Wang, J. (2000) *Biochemistry* **39,** 12424–12434
46. Das, T. K., Gomes, C. M., Teixeira, M., and Rousseau, D. L. (1999) *Proc. Natl. Acad. Sci. U. S. A.* **96,** 9591–9596
47. Han, S., Ching, Y-C., and Rousseau, D. L. (1990) *J. Am. Chem. Soc.* **112,** 9445–9451